Composite Structures 153 (2016) 876–885

Contents lists available at ScienceDirect

Composite Structures

journal homepage: www.elsevier.com/locate/compstruct

Analytical and finite element studies on behavior of FRP strengthened RC beams under torsion

Anand Ganganagoudar, Tarutal Ghosh Mondal, S. Suriya Prakash *

Department of Civil Engineering, Indian Institute of Technology Hyderabad, India

ARTICLE INFO

Article history:
Received 3 January 2016
Revised 26 May 2016
Accepted 6 July 2016
Available online 9 July 2016

Keywords:
Softened membrane model
Torsion
FRP strengthening
Tension stiffening effect
Finite element analysis
Confinement
Softening

ABSTRACT

This paper presents analytical and finite element (FE) studies on behavior of FRP (fiber reinforced polymer) composite strengthened reinforced concrete (RC) beams under torsional loading. Presence of torsion significantly changes the failure mode of RC members and therefore it is essential to understand the efficiency of FRP strengthening under torsion. This study tries to fill the knowledge gap existing in this important area of research by carrying out analytical and FE studies. An improved softened membrane model for torsion (SMMT-FRP) considering the influence of FRP composites on the compressive behavior of cracked concrete is proposed. A new tension stiffening relationship of concrete is also recommended for improved analytical predictions. The analytical study is accompanied by a full scale nonlinear FE study using commercial package ABAQUS. Parameters such as post cracking stiffness, peak torque and peak twist are accurately captured by the improved SMMT-FRP. Finite element predictions are also compared with analytical predictions and experimental results. Comparisons indicate a reasonably good agreement of both analytical and FE results with test data. FRP strengthening increased the post-cracking stiffness, ultimate strength and localized the damage.

1. Introduction

Fiber reinforced polymer (FRP) is a widely used strengthening material for reinforced concrete members owing to its various advantages such as light weight, ease of application, high strength and stiffness. Faulty design, unexpected loads, change in usage type, construction errors are few of the reasons which necessitate the strengthening of existing structures. The behavior of FRP strengthened reinforced concrete (RC) members is more complex than the unstrengthened RC members and therefore, a clear understanding of their behavior under different types of loading is important. A plethora of studies has been conducted in the past to understand the behavior of FRP strengthened RC beams under flexure and shear [1–2]. However, torsional behavior has not been given significant attention despite its frequent occurrence in many important engineering structures. Though torsion is considered as a secondary effect for most general cases, it becomes critical in cases such as connecting beams, outrigger bent, and bridge columns. Therefore, it is important to understand the behavior of RC members under torsional loading in detail. Moreover, the efficiency of FRP strengthening in terms of strength and stiffness improvement under torsional loading is relatively not very well understood. This is due to the complex nature of interaction effects of FRP on the softening and confinement of concrete and increased tension stiffening behavior of concrete. This study tries to fill the knowledge gap existing in this vital area of research by carrying out analytical and FE studies. Behavior of FRP strengthened RC beam can be understood from the assembly of membrane elements with additional equilibrium and compatibility conditions. Fig. 1 describes the shear flow in an FRP strengthened RC beam subjected an external torque '*T*'. Membrane element 'E' subjected to shear flow '*q*' is also shown in Fig. 1.

2. Review of literature

Few researchers in the past have experimentally investigated the behavior of FRP strengthened RC members under torsional loading. Ghobarah [3] experimentally studied the effect of CFRP (Carbon fiber reinforced polymer) and GFRP (Glass fiber reinforced polymer) strengthening on torsional behavior RC beams. Different wrapping configurations were used in this study and the authors concluded that 45 degree orientation of the fiber is more effective than 0 and 90 degree oriented configurations in increasing the torsional strength. Zhang et al. [4] investigated the torsional behavior

* Corresponding author.
E-mail addresses: ce14mtech11010@iith.ac.in (A. Ganganagoudar), ce13m1023@iith.ac.in (T.G. Mondal), suriyap@iith.ac.in (S. Suriya Prakash).

http://dx.doi.org/10.1016/j.compstruct.2016.07.014
0263-8223/

Nomenclature

A_0	the area enclosed by the centreline of shear flow
A_l	total cross-sectional area of longitudinal steel bars
A_t	cross-sectional area of one transverse steel bar
A_c	cross-sectional area bounded by the outer perimeter of the concrete
B	variable as defined in the constitutive relationship of embedded mild steel
E_c	elastic modulus of concrete
E_s	elastic modulus of the steel bars
f'_c	cylinder compressive strength of concrete
f_{cr}	cracking stress of concrete
f_l, f_t	smeared (average) steel stress in the longitudinal and transverse directions, respectively
f_s	smeared (average) stress of steel bars
f_n	smeared (average) yield stress of steel bars
f_0	projection of strain hardening of steel on Y-axis
f_p	smeared (average) ultimate stress of steel bars
f_y	yield stress and strain of bare steel bars
k_{2c}	ratio of the average compressive stress to the peak compressive stress in the concrete struts
k_{1c}	ratio of average tensile stress of the peak tensile stress in the concrete struts
P_0	perimeter of centreline of shear flow zone
P_c	perimeter of outer concrete cross section
q	shear flow
H	variable as defined to calculate the thickness of the shear flow zone
s	spacing of transverse bars
T	torque
t_d	thickness of shear flow zone
w	out-of-plane displacement in the direction normal to the membrane element
α	fixed angle, angle of applied principal compressive stress (2-axis) with respect to longitudinal steel bars
β	deviational angle
ε_0	concrete cylinder strain corresponding to peak compressive strength f_c
$\overline{\varepsilon_1}, \overline{\varepsilon_2}$	smeared (average) uniaxial strain in the 1 and 2-directions, respectively
$\varepsilon_1, \varepsilon_2$	smeared (average) biaxial strain in the 1 and 2-directions, respectively
$\overline{\varepsilon_l}, \overline{\varepsilon_t}$	smeared (average) uniaxial strain in the l and t directions, respectively
$\varepsilon_l, \varepsilon_t$	smeared (average) biaxial strain in the l and t directions, respectively
$\overline{\varepsilon_y}$	smeared (average) uniaxial yield strain of the steel bars
$\overline{\varepsilon_{2s}}$	maximum strain in concrete strut along 2 direction
$\overline{\varepsilon_p}$	smeared (average) failure strain of steel
$\overline{\gamma_{lt}}$	smeared (average) shear strain in the l-t coordinates of the steel bars
σ_1, σ_2	smeared (average) normal stresses of concrete in the 1 and 2 directions, respectively
σ_l, σ_t	applied normal stresses in the l and t directions of steel bars
τ_{12c}	smeared (average) shear stress of concrete in 1–2 coordinate
ρ_l, ρ_t	longitudinal and transverse steel ratios respectively
ν_{12}, ν_{21}	Hsu/Zhu ratios
θ	angle of twist per unit length
ψ	curvature of the concrete struts
ζ	softened coefficient of concrete in compression
t_{frp}	thickness of FRP sheets
E_{frp}	modulus of elasticity of FRP sheets

of RC beams using CFRP sheets as external reinforcement. Panchacharam and Belarbi [5] conducted an experimental study of the torsional behavior of RC beams strengthened with FRP composites. Number of plies, fiber orientation, and number of beam faces strengthened were the study parameters. Authors concluded that strengthening with GFRP sheets significantly increases ultimate strength and corresponding twist. They also noted that fibers oriented at 90 degrees to the beam axis provided the most effective confinement. Ronagh and Dux [6]; and Hii and Al-Mahiadi [7] also investigated the effect of FRP on the torsional behavior of RC members. They concluded that externally bonded CFRP increased cracking and ultimate strength by 40% and 78% respectively compared to control specimens. Jing and Grunberg [8] investigated the behavior of reinforced concrete box beams strengthened with CFRP sheets under combined action of bending, shear and torsion and proposed a mathematical model based on diagonal compression field theory. This model was basically developed for box beams subjected to low bending torque ratios and shear torque ratios. Ameli et al. [9] studied the effect of CFRP and GFRP on the torsional behavior of RC beams. The authors also performed a numerical study using ANSYS finite element software and concluded that the finite element model was able to capture the ultimate torque and discrepancy from the experimental observations are found to be less than 13% but post crack behavior is less accurately captured. He et al. [10] studied the effect of CFRP on behavior of damaged RC bridge columns that had fractured longitudinal bars. These columns were externally strengthened in both longitudinal and transverse directions. The authors found that strengthened columns were successful in regaining the strength of columns without fractured bars. He et al. [11] investigated the torsional behavior of RC damaged column strengthened with CFRP strips in both longitudinal and transverse directions. They found that CFRP strengthening was able to restore the strength and stiffness of damaged columns. Similar research was carried by Yang et al. [12]. The authors experimentally investigated the behavior of FRP strengthened RC bridge columns which had buckled longitudinal bars before strengthening. These strengthened columns were tested under constant axial load and cyclic lateral load that results the combined action of bending, shear, and torsion. The authors concluded that columns recovered their ability to perform against cyclic loading in terms of lateral strength and ductility. Chalioris [13] proposed an extended analytical model for FRP strengthened RC beams subjected to torsion for which classical softened truss

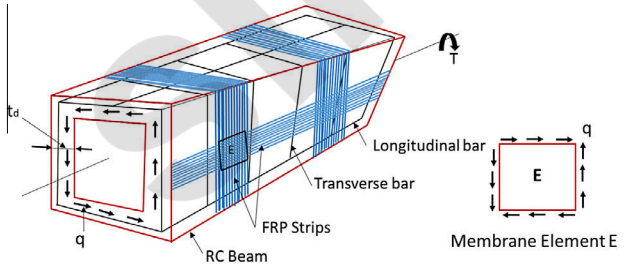

Fig. 1. FRP wrapped RC beam subjected to torsion and membrane element E.

model forms the basis. This model utilizes softened and FRP confined compression curve for concrete. Author concluded that the proposed model is found satisfactory in predicting the post crack stiffness. Moslehy et al. [14] studied the influence of FRP on the constitutive relationships of reinforced concrete elements. Researchers modified conventional softening coefficient to take the effect of FRP into account. Ganganagoudar et al. [15] investigated the torsional behavior of circular RC bridge columns under torsional loading. Authors proposed an improved SMMT for circular columns which considering the strain gradient effect and modified tension stiffening relationships. The present study is motivated from improving the existing analytical models by implementing better constitutive relationships of concrete in compression and tension. Experimental data available from the literature is used for comparison to check the validation of the results of proposed analytical and finite element models.

3. Research motivation and objectives

FRP wrapping of RC members produces confinement which stiffens the behavior of concrete struts under compression. The existing constitutive laws for concrete under compression do not take this confinement effect into account. This paper aims at filling this knowledge gap by proposing a modified concrete constitutive law under compression by incorporating this confinement effect. Besides, the confinement offered by FRP wrapping helps to control the cracking of concrete under tension. The present study recommends a new tension stiffening model for concrete for improved predictions of the torsional response of FRP strengthened beams. A nonlinear finite element model of FRP strengthened RC beams is developed and analyzed for various parameters to compare the predictions of analytical model and observe the damage progression. A combination of analytical and numerical studies gives a holistic understanding of this complex problem. The main objectives of the study are enumerated below:

i. To modify the constitutive law for concrete to take into account the confinement effect produced by FRP wrapping.
ii. To propose a new tension stiffening model for improved prediction.
iii. To develop a FE model which can predict the torsional response of FRP wrapped RC members and understand the global damage mechanisms which is otherwise not possible in SMMT-FRP model.

4. Improved softened membrane model for torsion with FRP (SMMT-FRP)

Softened membrane model for torsion was first proposed by Jeng and Hsu [16] for rectangular RC beams. In this study, it is extended to include the effect of FRP by considering a more realistic constitutive relationship of concrete in compression due to the effect of FRP strengthening. A new tension stiffening relationship is also employed for better predictions. It is worth mentioning that the underlying theory for the proposed model is based on the popular truss concept for cracked reinforced concrete, which was developed based on three Navier's principles of mechanics that are discussed in the following sections.

4.1. Navier's principles of mechanics

4.1.1. Equilibrium of stresses

Concrete is fully effective in resisting the applied torque before cracking. Once the applied torque reaches the cracking torque, steel and FRP become effective in resisting the applied torque. Membrane element subjected to in plane stresses and corresponding stress components of concrete, steel and FRP is shown in Fig. 2. Eqs. (1)–(3) represent the stress equilibrium equations for the membrane element.

$$\sigma_l = \sigma_{2c}\cos^2\alpha + \sigma_{1c}\sin^2\alpha + 2\tau_{12c}\sin\alpha\cos\alpha + \rho_l f_l + \rho_{fl} f_{fl} \tag{1}$$

$$\sigma_t = \sigma_{2c}\cos^2\alpha + \sigma_{1c}\sin^2\alpha - 2\tau_{12c}\sin\alpha\cos\alpha + \rho_t f_t + \rho_{ft} f_{ft} \tag{2}$$

$$\tau_{lt} = (-\sigma_{2c} + \sigma_{1c})\sin\alpha\cos\alpha + \tau_{12c}(\cos^2\alpha - \sin^2\alpha) \tag{3}$$

4.1.2. Compatibility of strains

Compatibility of strains between steel and concrete must be ensured. Eqs. (4)–(6) represent the compatibility conditions.

$$\varepsilon_l = \varepsilon_{2c}\cos^2\alpha + \varepsilon_{1c}\sin^2\alpha + \gamma_{12c}\sin\alpha\cos\alpha \tag{4}$$

$$\varepsilon_t = \varepsilon_{2c}\cos^2\alpha + \varepsilon_{1c}\sin^2\alpha - \gamma_{12c}\sin\alpha\cos\alpha \tag{5}$$

$$\frac{\gamma_{lt}}{2} = (-\varepsilon_{2c} + \varepsilon_{1c})\sin\alpha\cos\alpha + \gamma_{12c}(\cos^2\alpha - \sin^2\alpha) \tag{6}$$

4.1.3. Constitutive laws for materials

The constitutive relationship of concrete, steel and FRP are presented in the following sections.

4.1.3.1. Concrete in compression. In the present study, modified softened stress strain relationship of concrete in compression is used which includes the effect of FRP. Since Confinement effect due to the presence of FRP will counteract the softening effect, an additional coefficient f_4 (FRP) is used to account this effect based on the experiments conducted by Moslehy et al. [14] on FRP wrapped RC panels under biaxial loading. This coefficient is essentially a function of smeared principal tensile strain, modulus of elasticity and thickness of FRP sheets. The proposed model incorporates this improved constitutive model for concrete in compression to predict the torsional behavior of FRP strengthened RC members under torsional loading. Softening coefficient is a function of three variables, namely compressive strength of concrete (f'_c), principal tensile strain ($\overline{\varepsilon_2}$) and deviation angle (β) [17]. Expression for softening coefficient (ζ) and Confinement coefficient ($f_4(FRP)$) are given by Eqs. (7)–(9) represent the Smeared softened compressive stress strain relationship of concrete. Fig. 3(a) depicts the softened stress strain curve of concrete and also shows the effect of confinement on the stress strain relationship.

$$\beta = \frac{1}{2}\left(\tan^{-1}\left(\frac{\gamma_{12}}{\varepsilon_2 - \varepsilon_1}\right)\right) \tag{7a}$$

$$\zeta = \frac{5.8}{\sqrt{f'_c}}\frac{0.9}{\sqrt{1 + 400\overline{\varepsilon_2}}}\left(\frac{(1-\beta)}{24^0}\right) \tag{7b}$$

$$f_4(FRP) = \left[1 + \left(\frac{E_{FRP}}{6890}\right)\left(\frac{t_{FRP}}{0.27}\right)^{\frac{2}{3}}(\overline{\varepsilon_1})\right](1.12 - 16\overline{\varepsilon_1}) \tag{7c}$$

$$\sigma_{2c} = k_{2c}\zeta f_4(FRP) f'_c \tag{8}$$

$$k_{2c} = \left[\frac{\overline{\varepsilon_{2s}}}{\zeta\varepsilon_0} - \frac{(\overline{\varepsilon_{2s}})^2}{3(\zeta\varepsilon_0)^2}\right] \quad \left(\frac{\overline{\varepsilon_{2s}}}{\zeta\varepsilon_0} \leqslant 1\right) \tag{9a}$$

$$k_{2c} = \left[1 - \frac{\zeta\varepsilon_0}{3\overline{\varepsilon_{2s}}} - \frac{1}{3\overline{\varepsilon_{2s}}}\left(\frac{(\overline{\varepsilon_{2s}} - \zeta\varepsilon_0)^3}{(4\varepsilon_0 - \zeta\varepsilon_0)^2}\right)\right] \quad \left(\frac{\overline{\varepsilon_{2s}}}{\zeta\varepsilon_0} > 1\right) \tag{9b}$$

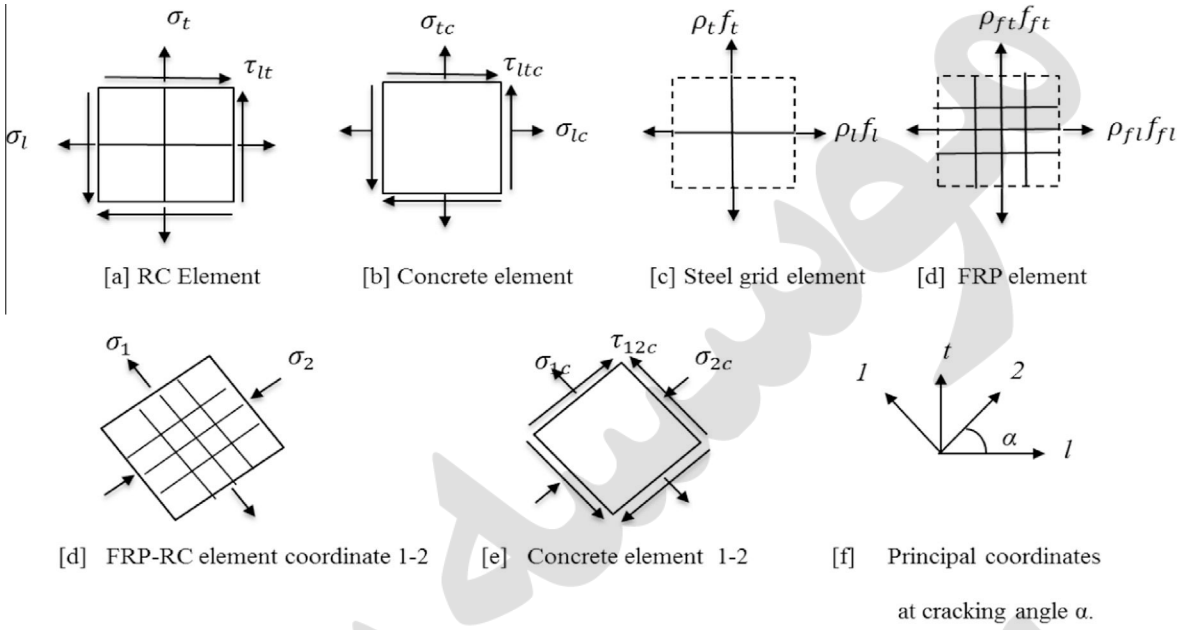

Fig. 2. FRP-RC membrane element subjected to in-plane stresses under torsion.

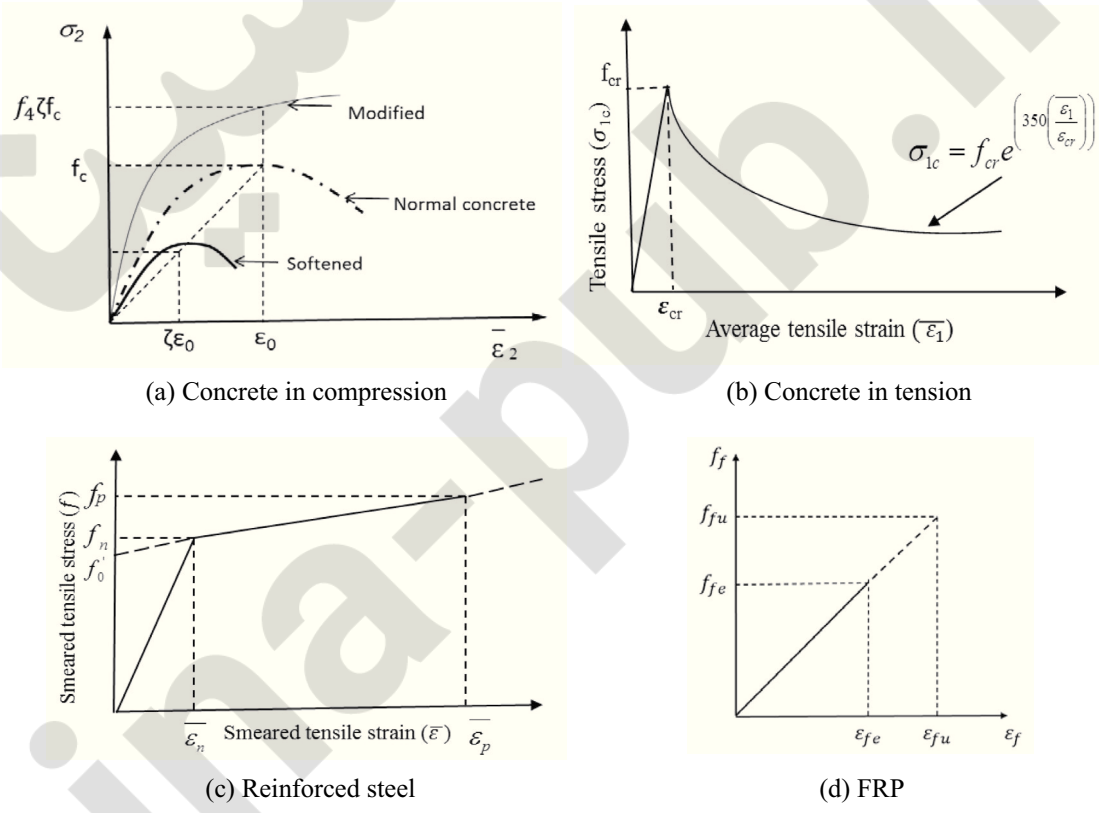

Fig. 3. Constitutive laws of materials.

4.1.3.2. Improved constitutive relationship for concrete in tension. Belarbi and Hsu [18] proposed a tension stiffening relation for concrete, which was later modified by Jeng and Hsu [16] to take the effect of strain gradient into account. In the present study, a new tension stiffening relationship is proposed by combining the models put forward by Jeng and Hsu [16] and Mondal and Prakash [19,20]. The cracking strength (Eq. (10a)) and initial tangent modulus (Eq. (10b)) have been adopted directly from Jeng and Hsu [16] model. Eqs. (11) and (12) represent the average stress factor for tension and ascending portion of the curves respectively. The descending part of the proposed model (Eq. (13)) resembles the exponential softening scheme proposed by Mondal and Prakash [19]. Fig. 3(b) represents the smeared stress strain curve of concrete under tension.

$$f_{cr} = 0.652\sqrt{f_{ck}} \tag{10a}$$

$$E_c = 5620\sqrt{f_{ck}} \tag{10b}$$

$$k_{1c} = \frac{1}{\overline{\varepsilon_{1s}} f_{cr}} \int_0^{\overline{\varepsilon_{1s}}} \sigma_{1c}(\overline{\varepsilon_1})\, d\overline{\varepsilon_1} \tag{11}$$

$$\sigma_{1c} = E_c \overline{\varepsilon_1} \sigma_{1c} = E_c \overline{\varepsilon_1} \quad \frac{\overline{\varepsilon_{1s}}}{\varepsilon_{cr}} \leqslant 1 \tag{12}$$

$$\sigma_{1c} = f_{cr} e^{(350(\varepsilon_{cr} - \overline{\varepsilon_1}))} \quad \frac{\overline{\varepsilon_{1s}}}{\varepsilon_{cr}} > 1 \tag{13}$$

4.1.3.3. Stress-strain relationship of steel and FRP. Fig. 3(c) shows smeared stress strain curve of steel embedded in concrete. The same material model was used for longitudinal (Eq. (14)) and transverse (Eq. (15)) steel. The behavior is assumed to be identical under tension and compression.

4.1.3.3.1. Longitudinal steel reinforcement.

$$f_1 = E_{sl} \overline{\varepsilon_l} \quad \overline{\varepsilon_l} < \overline{\varepsilon_{ln}} \tag{14a}$$

$$f_l = \left[(0.91 - 2B) + (0.02 + 0.25B) \frac{\overline{\varepsilon_l}}{\varepsilon_{ly}} \right] \quad \overline{\varepsilon_l} \geqslant \overline{\varepsilon_{ln}} \tag{14b}$$

$$B = \left[\frac{(f_{cr}/f_{ly})^{1.5}}{\rho} \right] \tag{14c}$$

$$\overline{\varepsilon_{ln}} = \varepsilon_{ly}(0.93 - 2B) \tag{14d}$$

4.1.3.3.2. Transverse steel reinforcement.

$$f_t = E_{st} \overline{\varepsilon_t} \quad \overline{\varepsilon_t} < \overline{\varepsilon_{tn}} \tag{15a}$$

$$f_t = \left[(0.91 - 2B) + (0.02 + 0.25B) \frac{\overline{\varepsilon_t}}{\varepsilon_{ty}} \right] \quad \overline{\varepsilon_t} \geqslant \overline{\varepsilon_{tn}} \tag{15b}$$

$$B = \left[\frac{(f_{cr}/f_{ty})^{1.5}}{\rho} \right] \tag{15c}$$

$$\overline{\varepsilon_{tn}} = \varepsilon_{ty}(0.93 - 2B) \tag{15d}$$

4.1.3.3.3. FRP. Fig. 3(d) shows stress strain behavior of FRP under uniaxial tension. The behavior is assumed to be linear elastic up to failure. Eq. (15e) shows the constitutive relationship FRP under tension.

$$f_{fe} = E_{frp} \varepsilon_{fe} \tag{15e}$$

4.1.4. Additional equations for torsion

4.1.4.1. Thickness of shear flow zone (t_d). Unlike rotating angle softened truss model (RA-STM), In SMMT, a simplified expression for t_d is proposed (Eq. (16)) to avoid the iterative calculations. Eqs. (16a) and (16b) represent the expressions for thickness of shear flow zone in terms of curvature (ψ) and curvature in terms of angle of twist (θ) respectively. Substitution and manipulation of Eqs. (16a) and (16b) yields an explicit expression for t_d (Eq. (16d)). A variable 'H' is used in calculation of 't_d' as shown in Eq. (16d).

$$t_d = \frac{\overline{\varepsilon_{2s}}}{\psi} \tag{16a}$$

$$\psi = \theta \sin 2\alpha_2 \tag{16b}$$

$$H = \frac{4\overline{\varepsilon_2}}{\gamma_{lt} \sin 2\alpha_2} \tag{16c}$$

$$t_d = \frac{1}{2(H+4)} \left[P_c \left(1 + \frac{H}{2}\right) - \sqrt{\left(1 + \frac{H}{2}\right)^2 - 4H(H+4)A_c} \right] \tag{16d}$$

Experimental investigation on establishing constitutive relationship for concrete in pure 2D shear is difficult. Establishing the same under torsional loading (3D shear) is furthermore difficult. Therefore, Hsu proposed an expression that relates the shear stress and shear strain in terms of normal stresses and strains (Eq. (17)).

$$\tau_{12c} = \frac{(-\sigma_{2c} + \sigma_{1c})}{2(\varepsilon_1 - \varepsilon_2)} \gamma_{12c} \tag{17}$$

The expressions for area (A_0) and perimeter (p_0) of shear flow zone are shown in Eqs. (18a) and (18b). Torque (T) and twist (θ) in the member can be calculated using the expressions given in Eqs. (19) and (20).

$$A_0 = A_c - \frac{p_c t_d}{2} + t_d^2 \tag{18a}$$

$$P_0 = P_c - 0.5 t_d \tag{18b}$$

$$T = 2A_0 t_d \tau_{lt} \tag{19}$$

$$\theta = \frac{P_0}{2A_0} \gamma_{lt} \tag{20}$$

Zhu and Hsu [21] proposed new parameters called Hsu/Zhu ratios to characterize the biaxial effect (Poisson's effect). The ratio was modified for torsion by Jeng and Hsu [16] to account for the strain gradient effect. Hsu/Zhu ratio for torsion was taken as 0.8 times the ratio used for shear (Eq. (22)). Uniaxial strains are written in terms of biaxial strains as shown in Eqs. (21a) and (21b).

$$\overline{\varepsilon_1} = \frac{\varepsilon_1}{(1 - \nu_{12}\nu_{21})} + \frac{\nu_{12}\varepsilon_2}{(1 - \nu_{12}\nu_{21})} \tag{21a}$$

$$\overline{\varepsilon_2} = \frac{\nu_{21}\varepsilon_1}{(1 - \nu_{12}\nu_{21})} + \frac{\varepsilon_2}{(1 - \nu_{12}\nu_{21})} \tag{21b}$$

$$\nu_{12} = (0.16 + 680\varepsilon_{sf}) \quad \varepsilon_{sf} \leqslant \varepsilon_y \tag{22a}$$

$$\nu_{12} = 1.52 \quad \varepsilon_{sf} > \varepsilon_y \tag{22b}$$

$$\nu_{21} = 0 \tag{22c}$$

4.1.5. Algorithm for SMMT-FRP

A strain controlled algorithm for SMMT-FRP, which includes the modified constitutive laws for concrete in compression and tension is presented in this section. The solution algorithm is implemented in MATLAB. Fig. 4 shows the solution algorithm of SMMT-FRP.

5. Experimental corroboration

For experimental validation of the proposed model, specimens tested by other researchers in the past were used. The details of the tested specimens are summarized in Table 1. Panchacharam and Belarbi [5] experimentally investigated the torsional behavior of FRP strengthened RC beams. Fiber orientation, wrapping configurations and number of faces strengthened were the study parameters of this research. Volumetric ratio of transverse reinforcement and longitudinal reinforcement was taken as 1%. Beams were square in cross section and closed stirrups were used as the

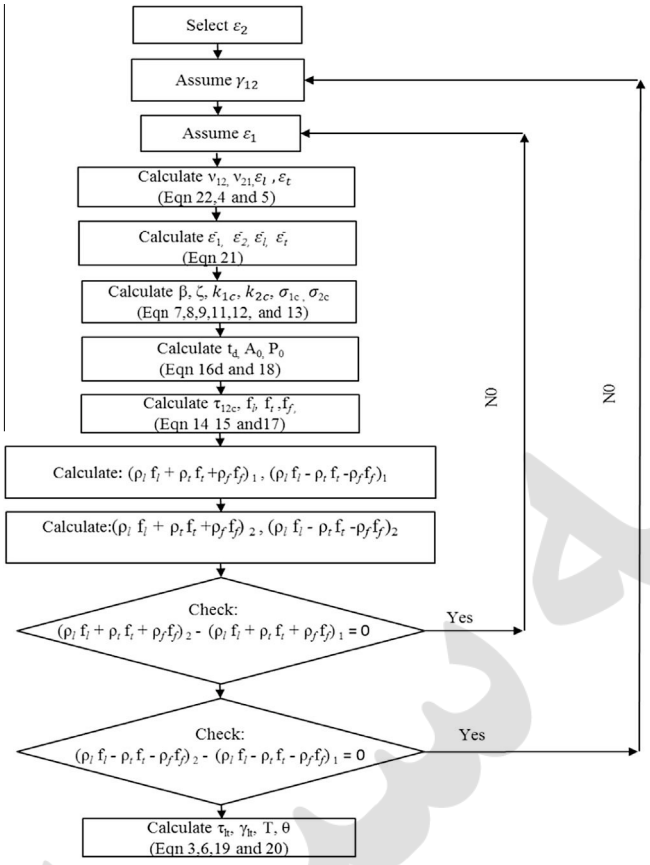

Fig. 4. Solution algorithm of SMMT-FRP.

transverse reinforcement. End zones of these beams were heavily reinforced in order to force the failure region to the middle zone. Authors investigated eight specimens out of which seven were strengthened with M-brace E-glass FRP sheets (unidirectional) and one was used as a control specimen. All eight beams were tested under pure torsion. Ultimate design strength and elastic modulus of GFRP sheets were 1520 MPa and 72 MPa respectively. Two specimens namely A90W4 and A90S4 were taken from this study to validate the proposed model. Details of these two specimens are listed in Table 1 and their experimental test setup is shown in Fig 5. It is worth mentioning that end boundary conditions allowed longitudinal expansion at the ends after cracking. Equal and opposite loads (P) apply a pure torsional moment in the RC beam (Fig. 5).

Another set of specimens is taken from the research conducted by Ameli et al. [9] to validate the proposed model. The authors investigated twelve FRP strengthened RC beams and out of which six were strengthened with GFRP and the rest were with CFRP sheets. MBrace CF130 and MBrace EG900 (unidirectional) were used as carbon and glass fibers respectively. Fiber configuration

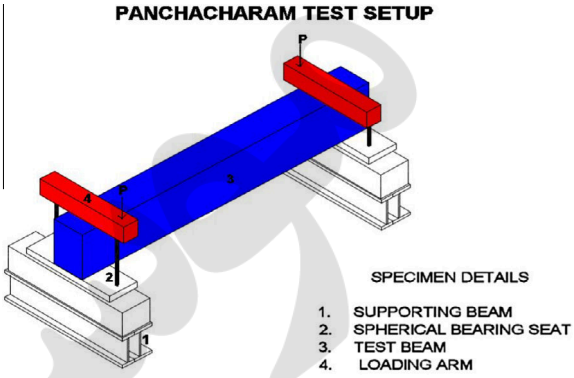

Fig. 5. Typical experimental Test setup for RC beams under torsion.

was a primary study parameter in this investigation. All specimens were essentially tested under pure torsional loading. Two specimens namely CFE and CFS taken from this study to validate the proposed model. Test details of representative specimens are reported in Table 1.

6. Finite element study

Finite element modelling of RC beams strengthened with FRP is much difficult as it should respond to different nonlinear behaviors such as cracking, crushing, yielding of steel, concrete plasticity, FRP debonding, and FRP rupture. Finite element investigation on RC beams subjected flexure and shear have been extensively carried out in the past by several researchers [22–24]. Despite its importance, very few researchers focused on the finite element study of the behavior of RC members under torsion. Mondal and Prakash [25] developed a nonlinear finite element model to predict the torsional behavior of RC bridge columns under combined action of torsion and axial compression. Authors carried out a parametric study by considering the amount transverse reinforcement and axial compression as the study parameters. Ameli et al. [9] proposed a finite element model for FRP strengthened RC beams. Authors concluded that the proposed model can efficiently capture the cracking torque and peak torque, but with reasonably less accurate prediction of the post crack stiffness. A nonlinear finite element model is proposed in this study to simulate the torsional behavior of FRP strengthened RC beams for various parameters using ABAQUS. Modelling details are discussed in the following sections in detail.

6.1. Concrete

Concrete is modelled using three dimensional eight node solid brick elements with three translational degrees of freedom at each node (C3D8R). Behavior of concrete in compression and tension are different. The damage plasticity approach is adopted to model the concrete [26]. Isotropic and linear elastic behavior of concrete both

Table 1
Details of the test specimens used for validation.

Beam	Cross section (mm^2)	f_c (MPa)	Stirrup diameter (mm)	Long. bar diameter (mm)	f_{ty} (MPa)	f_{ly} (MPa)	s (mm)	FRP type	Configuration of FRP
CFE	150 × 350	39	6	16	251	502	80	CFRP	One layer, fully wrapped
CFS	150 × 350	39	6	16	251	502	80	CFRP	One layer, Strips of 100 mm at 100 mm spacing
A90W4	279.4 × 279.4	34	9.5	9.5 and 12.7	420	460	152	GFRP	One layer, fully wrapped
A90S4	279.4 × 279.4	34	9.5	9.5 and 12.7	420	460	152	GFRP	One layer, strips at 150 mm at 150 mm spacing

in compression and tension are defined using Young's modulus and Poisson's ratio. Nonlinear behavior is defined in terms of inelastic strain and corresponding yield stress. Parabolic model is used to define the compressive stress-strain curve. Tension stiffening behavior is assumed for concrete under tension to appropriately model the post-cracking behavior. Concrete behaves elastically up to cracking point and thereafter the behavior is softened. Exponential model proposed by Greene [27] is used to model post-cracking behavior in tension. Failure ratios for concrete used in the model are reported in Table 2.

6.2. Steel

Longitudinal and transverse reinforcements are modelled with three dimensional, two noded truss elements (T2D3). Elastic perfectly plastic stress strain relationship is assumed for steel under both compression and tension. Steel being an isotropic material, linear elastic behavior is defined by elastic modulus and Poisson's ratio. Perfectly plastic behavior is defined using any two points on the yield line in terms of inelastic strain and yield stress.

6.3. FRP

FRP is generally considered as transversely isotropic material which is a subset of an orthotropic material. Lamina behavior in ABAQUS defines transversely isotropic material that requires five constitutive constants to define stress strain relationship unlike nine constants in orthotropic material. FRP (S4R) is modelled using three dimensional shell element.

6.4. Interaction

Concrete – steel interaction is modelled using embedded region constraint which is a built-in interaction in ABAQUS. Unlike flexure, under torsional loading bond slip between concrete and steel is insignificant [28]. Mondal and Prakash [25] investigated the effect of bond slip in torsional behavior of RC Bridge columns. Authors concluded that the effect of bond slip is trivial under torsional loading and assumption of perfecting bonding is a good approximation. Perfect bond is also assumed to define the interaction between Concrete and FRP for simplification using a tie constraint. Table 3 summarizes the type of element and material behavior used for all specimens. Element discretization of all three components is shown in Fig. 6.

6.5. Dynamic explicit scheme

Generally for nonlinear problems, explicit integration schemes are used in time marching algorithms [30]. Explicit integration techniques are good at convergence and more stable than implicit techniques. Any static problem can be treated as a subset of a dynamic problem because pure static cases are impractical. Therefore, the problem at hand can be considered as a quasi-static problem which possesses negligible inertia forces. For a quasi-static problem, total kinetic energy should be negligible compared to the internal energy of the system [30]. This condition was ensured in the present study for all specimens. Regarding loading and boundary conditions are concerned, one end of the beam is treated as fixed and twist about the member axis is applied at the other end. The simulation is carried out in displacement controlled scheme as it can better capture the post peak behavior. The problem is analyzed as a dynamic problem, and therefore the twist is applied with respect to time.

Table 2
Parameters for FE modelling.

Dilation angle	Eccentricity	Biaxial to uniaxial compressive strength ratio $\frac{f_{b0}}{f_{c0}}$	K	Viscosity parameter
36	0.1	1.16	0.67	0

Table 3
Element type and Idealized stress strain curve of materials.

Material	Element type	Idealized curve
Concrete	Solid-C3D8R	Parabolic
Steel	Truss-T3D3	Elastic–perfectly plastic
FRP	Shell-S4R	Elastic

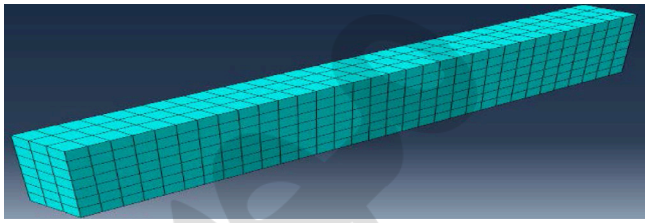

(a) Concrete

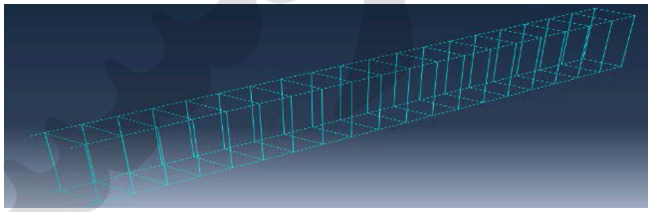

(b) Steel

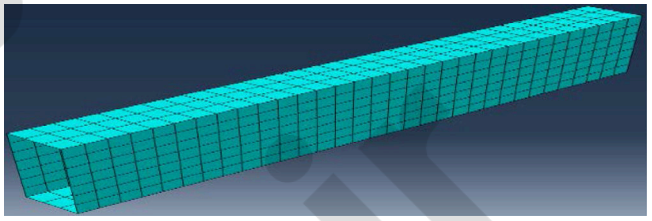

(c) FRP

Fig. 6. Finite element discretization of different components.

7. Results and discussions

Analytical and FEM results are discussed separately in the following sections. Analytical predictions are validated with the experimental results taken from literature and a good match was found. Predicted and experimental results for overall torque twist behavior are compared for all the specimens. Detailed discussion of the results is presented in the following sections.

7.1. Torque – twist behavior from SMMT-FRP and FE Study

Overall torque-twist behavior of the all beams predicted by model is presented in Fig. 7. It is observed that, post cracking behavior predicted by the model proposed in this study is close to the observed behavior. Average discrepancy of experimental peak torque, corresponding twist and the analytical predictions is less than 11% and 20%, respectively. The observed and predicted values of peak torque and peak twist are summarized in Table 4. Finite element model were created for all the four specimens and

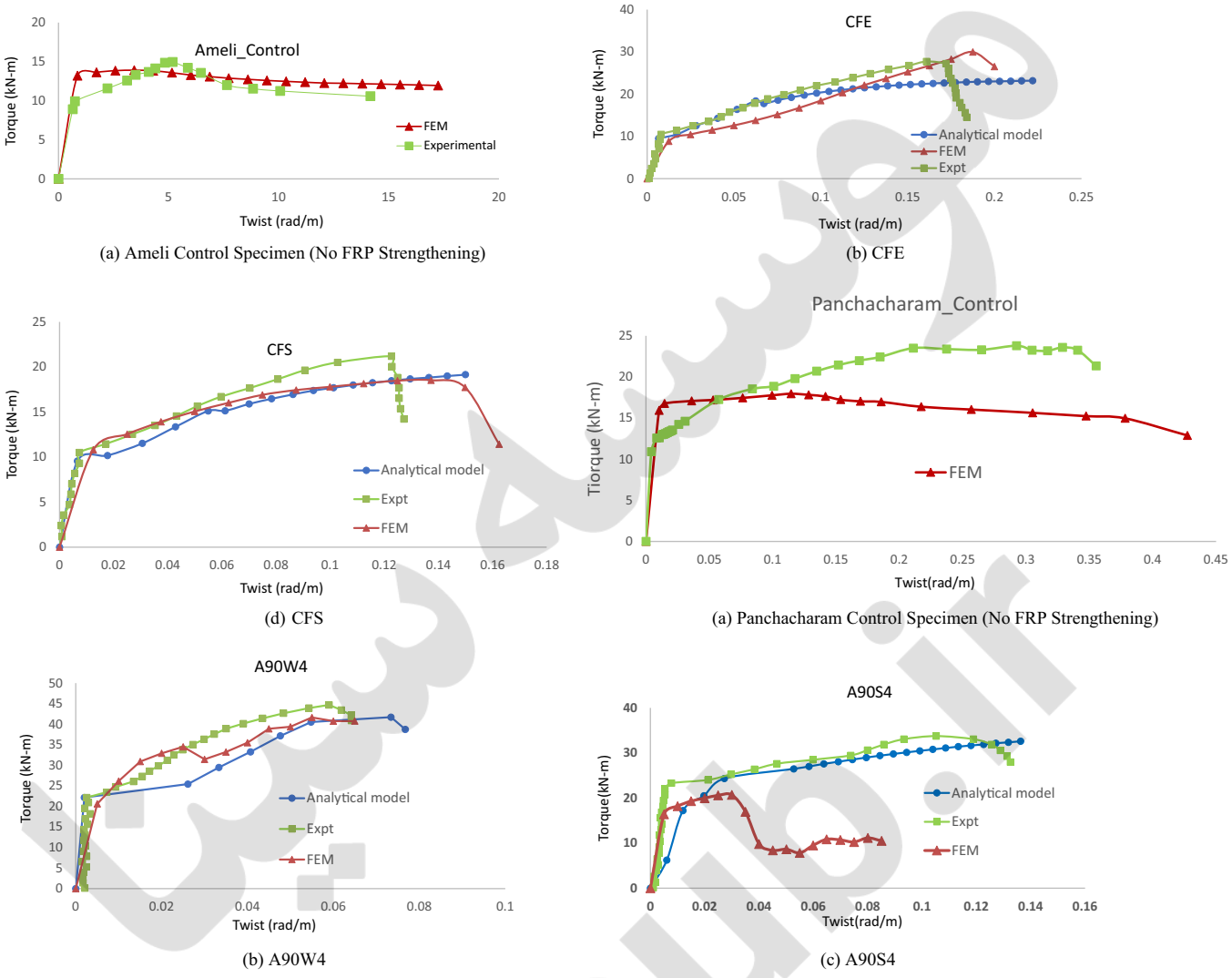

(a) Ameli Control Specimen (No FRP Strengthening)

(b) CFE

(d) CFS

(a) Panchacharam Control Specimen (No FRP Strengthening)

(b) A90W4

(c) A90S4

Fig. 7. Comparison of FEM and analytical results with experimental data.

Table 4
Comparison of analytical, FEM and experimental data.

Specimen ID/parameters	A90W4			A90S4			CFE			CFS		
	Exp.	FEM.	Predicted	Exp.	FEM.	Predicted	Exp.	FEM.	Predicted	Exp.	FEM	Predicted
Cracking torque (kN-m)	22.2	20.6	22.1	23.3	16.4	22.1	10.5	10.5	10.5	10.5	10.8	9.3
Cracking twist (rad/m)	0.0025	0.0050	0.0025	0.0070	0.0050	0.0052	0.008	0.024	0.008	0.007	0.0120	0.007
Peak torque (kN-m)	45.0	37.2	41.7	34.0	21.0	32.6	27.7	29.9	23.2	21.2	18.5	19.2
Peak twist (rad/m)	0.058	0.054	0.073	0.105	0.020	0.136	0.160	0.18	0.22	0.122	0.137	0.14
$T_{u,exp}/T_{u,FEM}$	NA	1.20	1.08	NA	1.61	1.04	NA	0.92	1.19	NA	1.14	1.13
θ_u,exp/θ_u,FEM	NA	1.07	0.80	NA	0.77	0.78	NA	0.89	0.72	NA	0.90	0.87

analyzed under pure torsional loading. Fig. 7 shows the comparison between experimental and finite element results of overall torque twist behavior. A reasonable match was found between the FE predictions and test data. The FE model accurately predicted the cracking torque (T_{cr}) and cracking twist (θ_{cr}). Peak values of torque and peak twist were also captured reasonably well. Average discrepancy in peak torque and corresponding twist values between experimental and FE predictions was found to be about 13% and 10% respectively. Considering the bond characteristics of FRP and concrete may yield better results and can be considered as the scope of further study. The effect of FRP is less significant before cracking of the concrete and this led to accurate prediction of the cracking torque and corresponding twist. However, the ultimate torque and corresponding twist were reasonably captured. Quantitative comparisons of FE model, analytical model and experimental results are reported in Table 4. Although the predictions from FEM and analytical models of peak capacity were reasonably close (less than 15% of average difference), there was a difference in the peak torque for one specimen (A90S4). The effect of boundary condition plays an important role in the predictions of finite element analysis. Longitudinal elongation of the beam was not restrained in the experimental study by provision of roller supports. However, there will be partial restraints offered by the supports and the FE models cannot accurately model this effect.

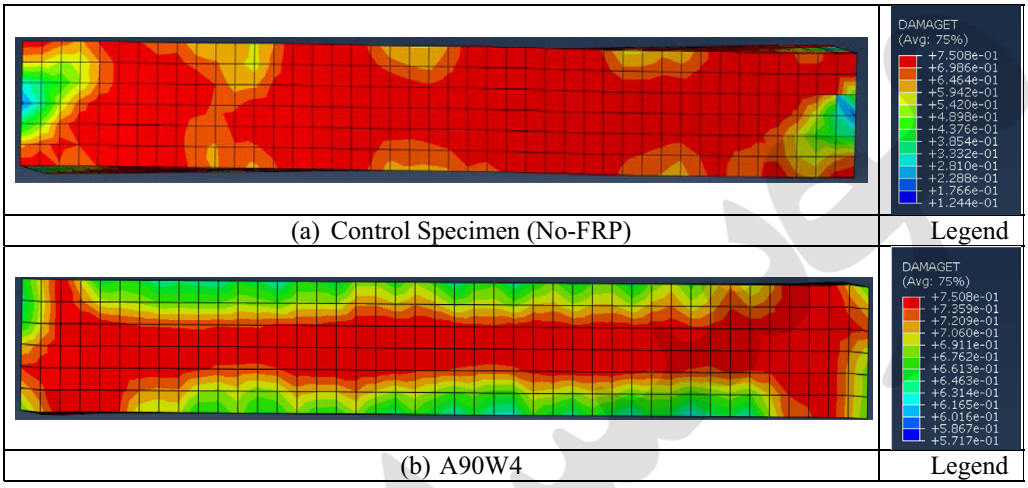

Fig. 8. Effect of FRP composite strengthening on damage distribution under torsion.

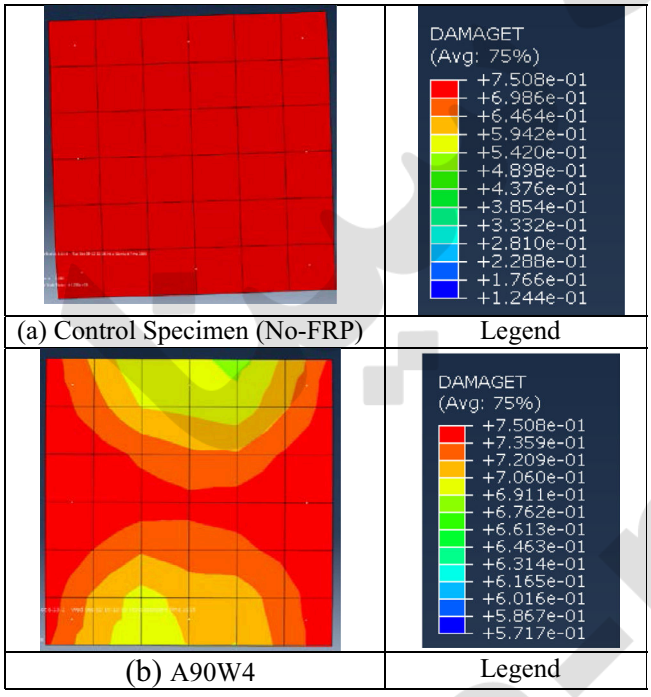

Fig. 9. Damage distribution across the cross section.

Moreover, the full wrapping of FRP composites significantly improves the torsional behavior in the experimental response by more efficiently arresting the crack propagation and reducing the softening of cracked concrete in compression. However, this improved tension stiffening and reduced softening of concrete is not properly considered in the FE model due to limitations in the formulation. It is worth mentioning that the analytical model proposed in the study consider these effects and thereby closely predicted the experimental response. Future work should focus on understanding the effect of full wrapping of FRP composites on improved tension stiffening and reduction in softening of cracked concrete in compression in the finite element formulations. Specimens considered for analysis had the following failure progression: shear cracking followed by yielding of transverse reinforcement and longitudinal reinforcement respectively. Specimens finally failed by crushing of the concrete under diagonal compression. The same failure progression was observed in both the analytical and finite element studies. Local debonding of FRP was not considered in the analytical and FE models. Debonding failure mechanism is very complex and considering its influence on the torsional behavior is scope for further work.

7.2. Damage distribution

In this section, damage distribution in FRP strengthened RC beam is compared with control (No FRP strengthening) beam. Damage index models have been developed in the past [29] for design purposes. The damage behavior of control and FRP strengthened beams is studied. Comparison for beam A90W4 and corresponding control (No FRP strengthening) specimen is presented to illustrate the difference in level of damage between strengthened and control beams. The control beam was identical to strengthened specimen in sectional details i.e., similar longitudinal reinforcement, transverse reinforcement and dimensions. The damage state observed at ultimate load is shown in Fig. 8. Tension damage variable (DAMAGET) is used for comparison to quantify the extent of damage in both the specimens. This variable ranges between zero and one where former value indicates the damage initiation and latter represents the complete damage. In other words, this parameter is a quantitative measure of material degradation (damage) under given loading condition damage contours clearly indicated that concrete cover spalling a major phenomenon in torsional behavior of RC beams was delayed due to external confinement provided by FRP strengthening. It can be clearly seen that, severity of damage in FRP strengthened beam (A90W4) is lesser than control (No FRP) specimen which confirms the contribution of FRP in resisting the damage progression. It is also observed that, FRP strengthening changes the damage distribution in beams by localizing the damage over a limited area.

Fig. 9 shows the damage distribution in the cross section for control specimen (NO FRP) and A90W4 specimen. It can be clearly seen that presence of FRP mitigates the damage in the cross section. Similar results were observed for other specimens as well.

8. Summary and conclusions

An improved analytical model is proposed to predict the torsional behavior of FRP strengthened RC members considering the effect of FRP confinement into account. More realistic constitutive relations of FRP strengthened concrete under torsional loading is employed in the proposed model. Together, a nonlinear FE model

is also developed in ABAQUS to capture the global torque–twist response and understand the failure progression. Major conclusions drawn from the study can be summarized as below.

1. Overall torque-twist behavior of the FRP strengthened RC beams were predicted closely by the proposed softened membrane model which included the effect of confinement, biaxial stress and strain gradient effect.
2. Peak torque and the corresponding twists and post-cracking behavior is better captured by the proposed analytical model.
3. Cracking torque and corresponding twist is accurately captured by proposed finite element model but with less accurate prediction of post-cracking behavior. Discrepancies in the peak torque between experimental and FE model was less than 13%.
4. Comparison of the FE and analytical predictions with test results validated that both the approaches were capable of predicting the behavior of FRP strengthened RC beams in torsion.
5. Concrete cover spalling was delayed due to external confinement provided by FRP strengthening.
6. Severity of damage in FRP strengthened specimens was significantly less compared to control specimens indicating the efficiency of FRP strengthening in Torsion. FRP strengthening localized the damage and resulted in better strength and stiffness increase.

Acknowledgements

This analytical work is carried out as part of the project funded by SERB, Department of Science and Technology, India. Grant No. SB/S3/CEE/0060/2013. Their financial support is gratefully acknowledged.

References

[1] Bonacci JF, Maalej M. Behavioral trends of RC beams strengthened with externally bonded FRP. J Compos Constr 2001;5(2):102–13.
[2] Pellegrino C, Modena C. Fiber reinforced polymer shear strengthening of reinforced concrete beams with transverse steel reinforcement. J Compos Constr 2002;6(2):104–11.
[3] Ghobarah A. FRP composites in civil engineering. Proc. FRP composites in civil engineering, CICE 2001, Hong Kong, vol. I. p. 701–12.
[4] Zhang JW, Lu ZT, Zhu H. Experimental study on the behavior of RC torsional members externally bonded with CFRP. FRP composites in civil engineering, proceedings of the international conference on FRP composites in civil engineering.
[5] Panchacharam S, Belarbi A. Torsional behavior of reinforced concrete beams strengthened with FRP composites. First FIB congress, Osaka, Japan, vol. 1. p. 01–110.
[6] Ronagh HR, Dux PF. Full-scale torsion testing of concrete beams strengthened with CFRP. Proc. 1st int. conf. on the performance of construction materials in the new millennium, Cairo, Egypt. p. 735–43.
[7] Hii AKY, Al-Mahaidi R. Torsional strengthening of reinforced concrete beams using CFRP composites. Proc. 2nd int. conf. on FRP composites in civil engineering, CICE 2004, Adelaide, Australia. p. 551–9.
[8] Jing M, Grunberg JX. Mechanical analysis of reinforced concrete box beam strengthened with carbon fiber sheets under combined actions. Compos Struct 2004;73(4):488–94.
[9] Ameli M, Ronagh HR, Dux PF. Behavior of FRP strengthened reinforced concrete beams under torsion. J Compos Constr 2007;11(2):192–200.
[10] He R, Grelle S, Sneed LH, Belarbi A. Rapid repair of a severely damaged RC column having fractured bars using externally bonded CFRP. Compos Struct 2013;101:225–42.
[11] He R, Sneed LH, Belarbi A. Torsional repair of severely damaged column using carbon fiber-reinforced polymer. ACI Struct J 2014;111(3):705–16.
[12] Yang Y, Sneed L, Saiidi MS, Belarbi A, Ehsani M, He R. Emergency repair of an RC bridge column with fractured bars using externally bonded prefabricated thin CFRP laminates and CFRP strip. Compos Struct 2015;133:727–38.
[13] Chalioris CE. Analytical model for the torsional behavior of reinforced concrete beams retrofitted with FRP materials. Eng Struct 2007;29(12):3263–76.
[14] Moslehy Y, Labib M, Ayoub A, Mullapudi R. Influence of fiber-reinforced polymer sheets on the constitutive relationships of reinforced concrete elements. J Compos Constr 2015 04015058.
[15] Ganganagoudar A, Mondal TG, Prakash SS. Improved softened membrane model for reinforced concrete circular bridge columns under torsional loading. J Bridge Eng 2016. http://dx.doi.org/10.1061/(ASCE)BE.1943-5592.0000907 04016037.
[16] Jeng CH, Hsu TT. Softened membrane model for torsion in reinforced concrete members. Eng Struct 2009;31(9):1944–54.
[17] Wang J. Constitutive relationships of pre-stressed concrete membrane elements [Ph.D. thesis]. Houston (TX, USA): Department of Civil and Environmental Engineering, University of Houston; 2006.
[18] Belarbi A, Hsu TT. Constitutive laws of concrete in tension and reinforcing bars stiffened by concrete. ACI Struct J 1994;91(4):465–74.
[19] Mondal TG, Prakash SS. Effect of tension stiffening on the behavior of reinforced concrete circular columns under torsion. Eng Struct 2015;92:186–95.
[20] Mondal TG, Prakash SS. Effect of tension stiffening on the behaviour of square RC columns under torsion. Struct Eng Mech J 2015;54(3):501–20 (Techno-press).
[21] Zhu RR, Hsu TT. Poisson effect in reinforced concrete membrane elements. ACI Struct J 2002;99(5):631–40.
[22] Ngo D, Scordelis AC. Finite element analysis of reinforced concrete beams. ACI J 1967;64(3).
[23] Lee HK, Kim BR, Ha SK. Numerical evaluation of shear strengthening performance of CFRP sheets/strips and sprayed epoxy coating repair systems. Compos B Eng 2008;39(5):851–62.
[24] Suriya Prakash S, Belarbi A, You YM. Seismic performance of circular RC columns subjected to axial, bending, and torsion with low and moderate shear. Eng Struct Elsevier 2010;32(1):46–59.
[25] Mondal TG, Prakash SS. Nonlinear finite-element analysis of RC bridge columns under torsion with and without axial compression. J Bridge Eng 2015. http://dx.doi.org/10.1061/(ASCE)BE.1943-5592.0000798 04015037.
[26] Fink J, Petraschek T, Ondris L. Push-out test parametric simulation study of a new sheet-type shears connector. Projekte an denzentralen Applikationsservern, Berichte, Zentraler Informatikdienst (ZID) der Technischen Univ. Wien, Wien, Austria, 2006. p. 131–153.
[27] Greene GG. Behavior of reinforced concrete girders under cyclic torsion and torsion combined with shear: Experimental investigation and analytical models [Ph.D. thesis]. Rolla, MO: Dept. of Civil, Architectural, and Environmental Engineering, Univ. of Missouri; 2006.
[28] Hurtado G. Effect of torsion on the flexural ductility of reinforced concrete bridge columns [Ph.D. thesis]. Berkeley, CA: Department of Civil and Environmental Engineering, University of California; 2009.
[29] Belarbi A, Prakash SS, Silva PF. Incorporation of decoupled damage index models in the performance-based evaluation of RC circular and square bridge columns under combined loadings, vol. 271. ACI Special Publication-SP271; 2010. p. 79–102.
[30] Zimmermann S. Finite Elemente und ihre Anwendung auf physikalischund geometrisch nichtlineare Probleme. Rep. TUE-BCO 01.05. Eindhoven, Netherlands: Eindhoven Univ. of Technology; 2001 (in German).